

New Behavior Model and Adaptive Predistortion for Power Amplifiers

Mingming Gao^{1, 2}, Yue Wu^{1, *}, Shaojun Fang², Jingchang Nan¹, and Shuyang Cui¹

Abstract—A three-box model, composed of a triangular memory polynomial, a look-up table, and a cross item among memory times, is proposed for power amplifiers. The model acquired good accuracy and linear effect and reduced the calculation coefficient. Moreover, the paper proposes the GRLS_IVSSLMS adaptive predistortion algorithm. This algorithm is based on the structure of indirect learning. This work uses 16QAM signal to drive a strongly nonlinear Doherty amplifier. Experimental results show that the proposed method is suitable for the adaptive predistortion of power amplifiers.

1. INTRODUCTION

With the development of modern communication technology, power amplifier (PA) devices produce strong nonlinearity and memory effects. Predistortion method is proposed for PA, and popular predistortion models are mainly polynomial, neural network, and look-up table (LUT) [1–3]. Polynomial predistortion models include Wiener-Hammerstein model, Volterra series model, and simplified memory polynomial models. The predistortion models based on LUT [4] are two-dimensional, multidimensional, and filter LUT models [5, 6]. Ref. [7] proposed a polynomial model, whereas [8] proposed the general polynomial model. However, the above predistortion algorithms face the same problem in which the PA model cannot be accurately estimated. The DPD (Digital Pre-Distortion) technology can compensate the nonlinear distortion of PA and memory effect by adopting the adaptive algorithm for baseband signal processing part, which requires the use of predistortion parameter identification algorithm for real-time update. Refs. [9–11] included different improvements on existing adaptive algorithms but still have the shortcomings of computational complexity, real-time and deficient factors of noise resistance, low convergence, and large mean square error. A good algorithm is necessary to improve the effect of predistortion linearization [12].

The remainder of this paper is organized as follows. In Section 2, from the perspective of simplifying the PA model, we propose a new simplified three-box PLTC (parallel-LUT-triangular memory polynomial (TMP)-CIMT) model for the behavioral model of nonlinear PA with memory effect and introduce an identification process. In Section 3, an adopting adaptive algorithm GRLS_IVSSLMS is proposed. The PA behavior model uses PLTC model, and the predistortion algorithm utilizes GRLS_IVSSLMS algorithm for this paper to achieve a good balance between modeling accuracy and predistortion algorithm complexity in Section 4. Finally, Section 5 concludes the paper.

Received 28 November 2018, Accepted 8 April 2019, Scheduled 31 May 2019

* Corresponding author: Yue Wu (1612252170@qq.com).

¹ School of Electronics and Information Engineering, Liaoning Technical University, Huludao 125105, China. ² School of Information Science and Technology, Dalian Maritime University, Dalian 116026, China.

2. PROPOSED MODEL

2.1. PA Three-Box Behavior Model

The PLTC model consists of LUT, a TMP, and cross-term memory timing signals in a parallel form. The model obtains a high accuracy by introducing the cross-term of current signals and lagged envelope. The block diagram of the model is illustrated in Figure 1.

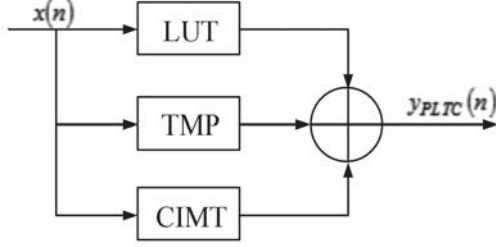


Figure 1. The block diagram of the PLTC model.

The first sub-model uses a high-order nonlinear function with memoryless. The PLTC model increases LUT to represent a static strong nonlinearity and reduces the complexity of the entire model. In this work, suppose that x/y is the input and output signals of the first sub-model, K_a a nonlinear order, and a_k the amplitude. The mathematical expression is written as:

$$y_{LUT}(n) = \sum_{k=1}^{K_a} a_k x(n) |x(n)|^{k-1} \quad (1)$$

The second sub-model is the TMP function that describes the nonlinear characteristic of an amplifier system. This sub-model is defined by the following formula:

$$y(n) = \sum_{\substack{k=1 \\ k\text{-odd}}}^K \sum_{q_k=0}^Q h_k(q_k) x(n - q_1) \prod_{m=1}^{(k-1)/2} x(n - q_{2m}) x^*(n - q_{2m}) \quad (2)$$

where k is the number of nonlinear order, q_k the memory depth, $h_k(q_k)$ the k -order Volterra kernel, and $k = 1, 3, \dots, K \cdot q_k = 0, 1, \dots, Q$. The MP is expressed as

$$y(n) = \sum_{k=1}^K \sum_{q=0}^Q a_{kq} x(n - q) |x(n - q)|^{k-1} \quad (3)$$

We can attempt to adjust the maximum nonlinear order of the input signal in the past while maintaining the performance of the predistortion and reducing the number of its coefficients. Let $K = N$, and N is defined:

$$N = \begin{cases} K - q; & q < K \\ 1; & q \geq K \end{cases} \quad (4)$$

From the formula, we can achieve:

$$y_{TMP}(n) = \sum_{q=1}^Q \sum_{k=1}^N a_{kq} x(n - q) |x(n - q)|^{k-1} \quad (5)$$

In Formula (4), the maximum nonlinear order is intermittent and changes with the memory depth variations. The TMP model overcomes the characteristics that model coefficients exponentially grow with nonlinear order and memory depth, and increase the historic moment for the current input signal envelope impact items.

The third sub-model is represented by the memory time signal cross-term CIMT function. The mathematical expression of this sub-model is:

$$y_{\text{CIMT}}(n) = \sum_{p=1}^M \sum_{\substack{q=1 \\ q \neq p}}^M \sum_{r=1}^N c_{pqr} x(n-p) |x(n-q)|^{r-1} \quad (6)$$

The increased CIMT model cross-term order will lead to the rapid growth of model coefficients. Considering that the high-order nonlinearity of memory time signals slightly impacts the system, we only consider the impact on the system of three-order intermodulation of the memory timing between signals. Formula (6) is simplified as:

$$y_{\text{CIMT}}^*(n) = \sum_{p=1}^M \sum_{\substack{q=1 \\ q \neq p}}^M c_{pq} x(n-p) |x(n-q)|^2 \quad (7)$$

Based on the above analysis, the PLTC model is given as follows:

$$y_{\text{PLTC}}(n) = \sum_{\substack{k=1 \\ k\text{-odd}}}^{K_a} a_k x(n) |x(n)|^{k-1} + \sum_{q=1}^Q \sum_{\substack{k=1 \\ k\text{-odd}}}^N a_{kq} x(n-q) |x(n-q)|^{k-1} \\ + \sum_{p=1}^M \sum_{\substack{q=1 \\ q \neq p}}^M c_{pq} x(n-p) |x(n-q)|^2 \quad (8)$$

The LUT represents the high-order static nonlinear behavior of the PA. The TMP sub-model uses low-order nonlinearity and controls the size of each model separately to form a reasonable number of total coefficients. This model avoids defects in selecting the same nonlinear order in each sub-model, which will increase calculation complexity and size of the model. Therefore, the PLTC model can reduce the size of the model by adding parallel nonlinear sub-models.

2.2. Identification PLTC Model

The PLTC model identification is divided into three steps. First, the high-order memoryless nonlinear static sub-model parameter is identified by the input and output data of the PA. Second, the TMP sub-model parameters are identified. Third, the CIMT sub-model parameters are identified. The TMP sub-model synchronization with the CIMT sub-model is identified as follows:

$$Y = X \cdot A \quad (9)$$

where Y is the output vector of two dynamic nonlinear polynomial sub-models, X the matrix of two polynomial basis functions of the input signal, and A the vector that contains the coefficients of the TMP and CIMT sub-model. Matrix X is defined as: $X = [X_{\text{TMP}}, X_{\text{CIMT}}]$. The matrix size X_{TMP} is $K \times ((M_{\text{TMP}} + 1) \times N_{\text{TMP}})$ and:

$$X_{\text{TMP}} = [X_{\text{TMP}1,l}(x(n_0 + 1)) \cdots X_{\text{TMP}k,l}(x(n_0 + k))]^T \quad (10)$$

k is the length of the vector and $k = 1000$. $X_{\text{TMP},l}$ is defined as:

$$X_{\text{TMP}k,i+(j \times N_{\text{TMP}})}(x(n_0 + k)) = x((n_0 + k) - j) \times |x((n_0 + k) - j)|^{i-1} \quad (11)$$

j is scanned from 0 to M_{TMP} , and i is scanned from 0 to N_{TMP} . Similarly, X_{CIMT} is defined as:

$$X_{\text{CIMT}k,i+(j \times N_{\text{CIMT}})}(x(n_0 + k)) = x(n_0 + k) \times |x((n_0 + k) - j)|^{i-1} \quad (12)$$

Finally, the least squares fitting method is used to calculate A . $[\]^H$ is the conjugate transposition.

$$A = (X^H \cdot X)^{-1} \cdot X^H \cdot Y \quad (13)$$

The accuracy of each model is measured with normalized mean square error (NMSE). A low NMSE is obtained by selecting low coefficient model dimensions. The sub-model is determined by the size of the general scanning method.

$$\text{NMSE}_{\text{dB}} = 10 \log_{10} \left(\frac{\sum_{n=1}^K |y_{\text{means}}(n) - y_{\text{est}}(n)|^2}{\sum_{n=1}^K |y_{\text{means}}(n)|^2} \right) \quad (14)$$

3. PROPOSED ALGORITHM

The DPD technology can compensate the nonlinear distortion of PA and memory effect by adopting adaptive algorithms [13–15], which use predistortion parameter identification algorithms for real-time update. This paper introduces an improved adaptive algorithm for DPD, which adopts the structure of indirect learning.

3.1. I_VSSLMS Algorithm

The VSSLMS (variable step size least mean square) algorithm is a class of LMS algorithms with variable step sizes, which overcomes the contradiction between convergence speed and the steady-state error of fixed step size LMS. In this paper, we propose a new VSSLMS, in which $X(n)$ and $d(n)$ stand for the input and output signals; $W(n)$ represents the tap coefficient of the filter; and $e(n)$ is the error signal. The VSSLMS algorithm is expressed as follows.

$$e(n) = d(n) - X^T(n)W(n) \quad (15)$$

$$W(n+1) = W(n) + \mu(n)e(n)X(n) \quad (16)$$

where $\mu(n)$ is the variable step size, and the relationship of the updating steps is expressed by Formula (17).

$$\mu(n+1) = \begin{cases} \mu_{\min} & \mu(n) < \mu_{\min} \\ \alpha\mu(n) + \beta e^2(n) & \text{other} \\ \mu_{\max} & \mu(n) > \mu_{\max} \end{cases} \quad (17)$$

In Formula (17), α determines the convergence step, and it is approximately 1; β determines the degree of influence in error transient energy of the steps and controls the steady-state error and convergence time, and $0 < \beta < 1$. μ_{\max} is the maximum possible convergence rate step size, and the approximate value of μ_{\max} is minimal, approximately $\frac{1}{\lambda_{\max}}$. λ_{\max} is the largest eigenvalue of the correlation matrix of the input signal. μ_{\min} is the minimum step, which has the ability to track. $e(n)$ is approximately zero, and $\beta e^2(n)$ is also close to zero. Hence, the VSSLMS algorithm ensures that the steady-state error is minimal and that it has a rapid convergence rate and time-varying tracking ability, but is susceptible to noise interference.

The VFSSLMS algorithm is an improved VSSLMS algorithm. $p(n)$ is the estimation error of $e(n)$ and $e(n-1)$. When the iteration step changes with the average time domain autocorrelation estimate of $e(n)$ and $e(n-1)$, this step is unaffected by uncorrelated noise impact. The VFSSLMS step algorithm for updating is as follows:

$$\mu(n+1) = \begin{cases} \mu_{\min} & \mu(n) < \mu_{\min} \\ \alpha\mu(n) + \beta p^2(n) & \text{other} \\ \mu_{\max} & \mu(n) > \mu_{\max} \end{cases} \quad (18)$$

$$p(n) = \gamma p(n-1) + (1-\gamma)e(n)e(n-1) \quad (19)$$

where $0 < \gamma < 1$ controls the convergence time, $\mu(0) = \mu_{\max}$, and $p(0) = \mu(0)$. We can ensure that a faster convergence rate is observed in the initial stage of the adaptive. β is used for controlling the steady-state error of the algorithm and convergence time. However, the noise affects β and makes the step length relatively large. Adding to the time-varying β , which changes with the error signal, this paper proposes the idea of an improved I_VSSLMS algorithm. The expression is as follows.

$$\beta(n) = [e(n)e(n-1)]^2 \quad (20)$$

$$\mu(n+1) = \begin{cases} \mu_{\min} & \mu(n) < \mu_{\min} \\ \alpha\mu(n) + \beta(n)e^2(n) & \text{other} \\ \mu_{\max} & \mu(n) > \mu_{\max} \end{cases} \quad (21)$$

First, β is large and can obtain a high step value influenced by the error signal. When the algorithm gradually turns into a steady state, β decreases with the declining error signal, and β obtains a low step value to ensure a steady state. When the system impulse response changes, the error signal rapidly changes, and the influence of β enlarges, which makes the step length change quickly in order to sustain the change of the system with the change of the system. We illustrate the algorithm performance by experiment.

The steps of the performance verification of the adaptive filter algorithm are as follows: (1) adaptive filter order $L = 2$; (2) signal $X(n)$ is a white Gaussian noise of zero mean with a variance of 1; (3) $v(n)$ and $X(n)$ are associated with the white noise sequence with zero mean, and variance is 0.04; (4) algorithm sampling for 1000 times; the coefficient of the unknown system changes $w_1 = [0.8, 0.5]^T$ into $w_2 = [0.4, 0.2]^T$ for 500 times; the VSS_LMS algorithm parameters take $\alpha = 0.98, \beta = 0.08, \gamma = 0.98, \mu_{\max} = 0.2, \mu_{\min} = 0$. To obtain a learning curve, 200 independent simulations are required with sampling for 2000 times, and then the mean square error is calculated.

In Figure 2, the VSS_LMS algorithm convergence speed is fast, but the steady-state error is also large. The VFSS_LMS algorithm steady-state error is minimal but is slow in time-varying tracking. The LVSS_LMS algorithm convergence speed is fast, and its steady-state error is minimal.

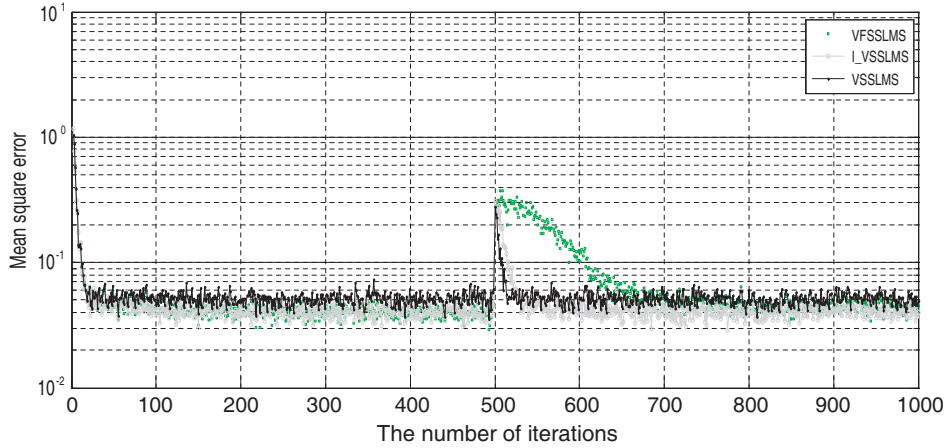


Figure 2. VSS_LMS algorithms learning curve comparison chart.

3.2. Improved RLS Algorithm

The RLS algorithm has the advantages of rapid convergence and minimal steady-state offset error, but its computing cost is relatively large and unstable when the error signal is less. Thus, improving the traditional RLS algorithm is necessary. The cost function of RLS is as follows.

$$F(e(n)) = \sum_{i=0}^n \lambda^{n-i} e^2(n) = \sum_{i=0}^n \lambda^{n-i} [d(n) - X^T(n)W(n)]^2 \quad (22)$$

where λ is known as the forgetting factor, and $0 < \lambda < 1$. The RLS algorithm weight vector iteration formula is:

$$W(n) = W(n-1) + K(n)e(n) \quad (23)$$

$$K(n) = \frac{R^{-1}(n-1)X(n)}{\lambda + X^T(n)R^{-1}(n-1)X(n)} \quad (24)$$

where $K(n)$ is the Kalman gain vector. The B_RLS algorithm is based on basic variable forgetting factor, which solves the contradiction between convergence speed and steady-state error. The B_RLS algorithm is expressed as:

$$\lambda(n) = \lambda_{\min} + (1 - \lambda_{\min}) \cdot 2^{L(n)} \quad (25)$$

$$L(n) = -\text{round}[\rho e^2(n)] \quad (26)$$

where $\text{round}(\cdot)$ is the nearest integer, and ρ controls the sensitivity of the estimation error. First, $e(n)$ is large, and $\lambda(n)$ is λ_{\min} to ensure rapid tracking. When the system is stabilized, $e(n)$ is smaller, and $\lambda(n)$ is 1 to ensure a minimal steady-state error. When the system is unknown, $K(n)$ trends become 0, and then the system is not updated.

A self-perturbation term becomes the Z_RLS algorithm through the inverse covariance matrix $P(n)$, avoiding $K(n)$ becoming 0. The formula to update $P(n)$ is as follows.

$$P(n) = \frac{1}{\lambda} \{P(n-1) - K(n)X^T(n)P(n-1) + \text{round}[\gamma e(n)]\} \quad (27)$$

where γ is the sensitive factor by taking $\gamma = 1$, and $\text{round}[\gamma e(n)]$ is the nearest integer to $\gamma e(n)$. Adopting $e(n)$ as a self-disturbance, this phenomenon makes the algorithm concise. Given that the expectations $e(n)$ and noise signal unrelated, this condition enhances the anti-noise interference ability of the Z_RLS algorithm. This paper proposes an improved RLS algorithm (G_RLS), which combines genetic factor and disturbance.

The G_RLS algorithm adjusts λ through function $\log \text{sig}(\cdot)$. λ increases with the number of trainings while strengthening the tracking ability and reducing the estimation error. In this work, the change of λ related to the number of iterations ignores the error signal, and the algorithm is slightly susceptible to the effects of interference noise. The forgetting factor is expressed as Formula (28).

$$\lambda(n) = \lambda_{\min} + (1 - \lambda_{\min}) \times \log \text{sig}(n/M) \quad (28)$$

where n is the number of iterations; M is an integer; λ_{\min} , n , and M can be obtained by the experiment. The function $y = \log \text{sig}(x)$ is expressed by Formula (29) and illustrated by Figure 6.

$$y = 1/1 + e^{-x} \quad (29)$$

In Figure 3, the iteration is few, and λ is minimal, making the convergence of the algorithm fast. When the algorithm converges into a steady state with the increase of the number of iterations, λ is large, and the steady-state error is minimal.

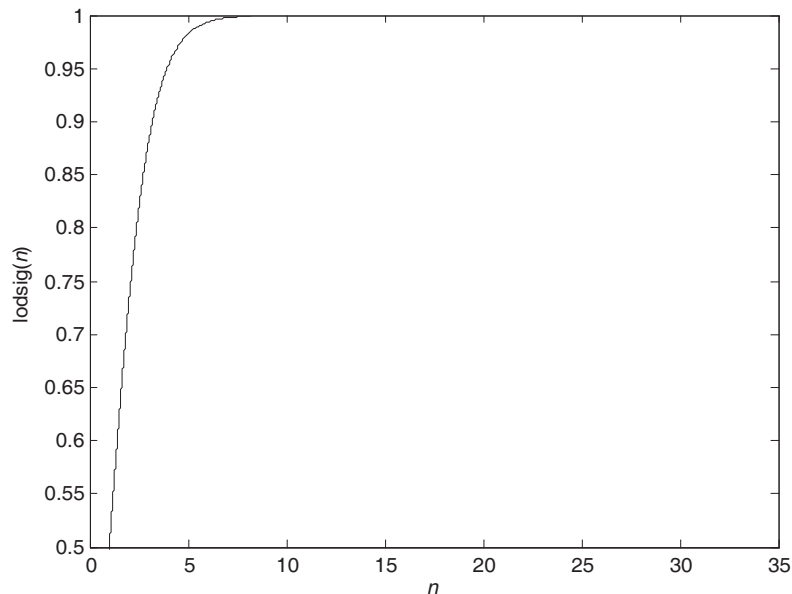


Figure 3. Curve of function $\log \text{sig}(n)$.

The improved G_RLS algorithm is combined with the Z_RLS algorithm, and the improved forgetting factor method can obtain good convergence speed and steady-state error performances. The G_RLS algorithm is expressed as follows.

$$\lambda(n) = \lambda_{\min} + (1 - \lambda_{\min}) \times \log \text{sig}(n/M) \tag{30}$$

$$P(n) = \frac{1}{\lambda(n)} \{P(n - 1) - K(n)X^T(n)P(n - 1) + \text{round}[\gamma e(n)]\} \tag{31}$$

The learning curve comparison chart of the RLS algorithm is illustrated in Figure 4. The parameter settings are described above, and the G_RLS algorithm $\lambda_{\min} = 0.95, M = 60$. The figure shows that the G_RLS algorithm is the best, since its convergence speed is the fastest, and the steady-state error is the smallest.

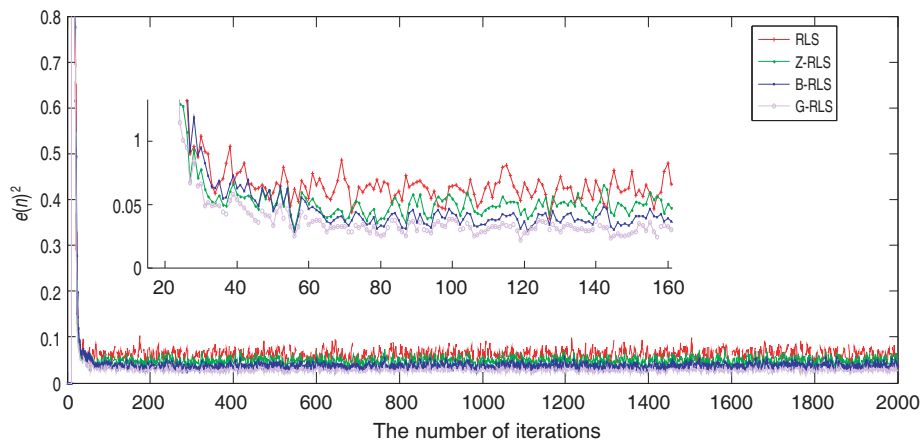


Figure 4. RLS algorithms learning curve comparison chart.

3.3. GRLS_IVSSLMS Algorithm

The RLS_LMS takes the advantages of both LMS and RLS algorithms; therefore, it has a rapid convergence rate and minimal steady-state error. This paper proposes the GRLS_IVSSLMS algorithm, which further improves the performance of the RLS_LMS algorithm and PD effect. The GRLS_IVSSLMS algorithm learning curve comparison chart is depicted in Figure 5. The RLS algorithm $\mu = 0.01, ET = 0.5$, and the LMS algorithm $\mu_{\max} = 0.65$. In the remaining parameters described above, the GRLS_IVSSLMS algorithm has a good convergence speed and steady-state misadjustment.

4. RESULT AND DISCUSSION

The design of the proposed adaptive algorithm is based on the initial stage of convergence or an unknown system parameter change. The step size should be relatively large to obtain rapid convergence speed and tracking speed time-varying systems. The algorithm converges should be kept minimal to achieve the small step size of the steady-state offset noise regardless of the primary input interfering signal $v(n)$.

The adaptive predistortion system block diagram of the GRLS_IVSSLMS algorithm is illustrated by Figure 6. The PA using the PLTC model and the PD algorithm using the GRLS_IVSSLMS select the G_RLS algorithm in the initial phase. After the steady-state of the G_RLS algorithm, the switch automatically receives the second side and converts to the IVSSLMS algorithm. When the error is more than the threshold, the algorithm switches to receive the first side, and then repeats the above process. The error signal threshold is important. Let $ET = |e(n)|$, the threshold ET is unaffected by other factors. The algorithm is only related to the error signal and can ensure stability.

In Figure 7, the spectrum inhibition of the GRLS_IVSSLMS PD algorithm has an obvious advantage over the RLS_LMS PD algorithm with an improved ACPR value of 3 dB. The ACPR value of the

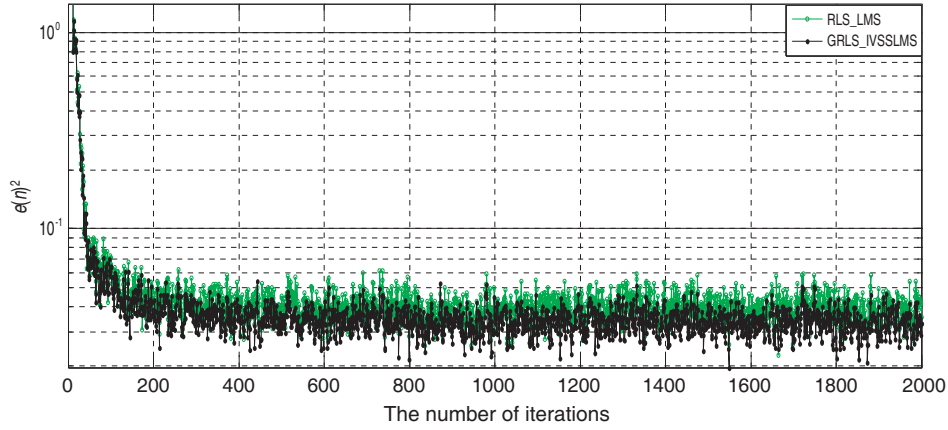


Figure 5. GRLS_IVSSLMS algorithm learning curve comparison chart.

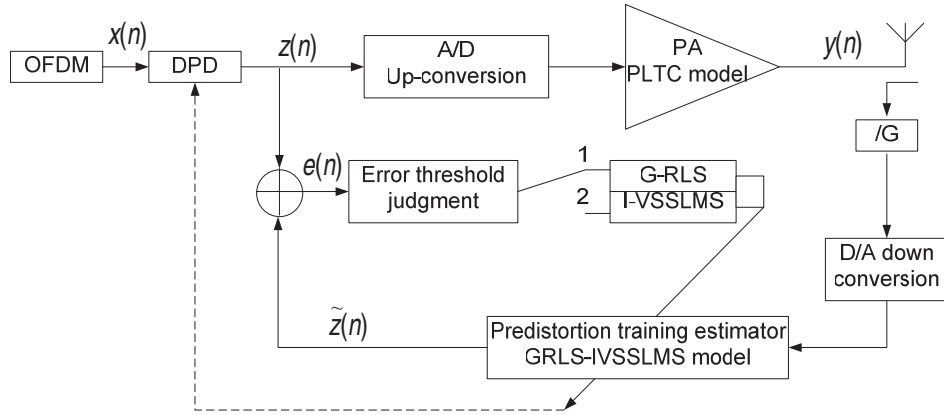


Figure 6. DPD system block diagram of the GRLS_IVSSLMS algorithm.

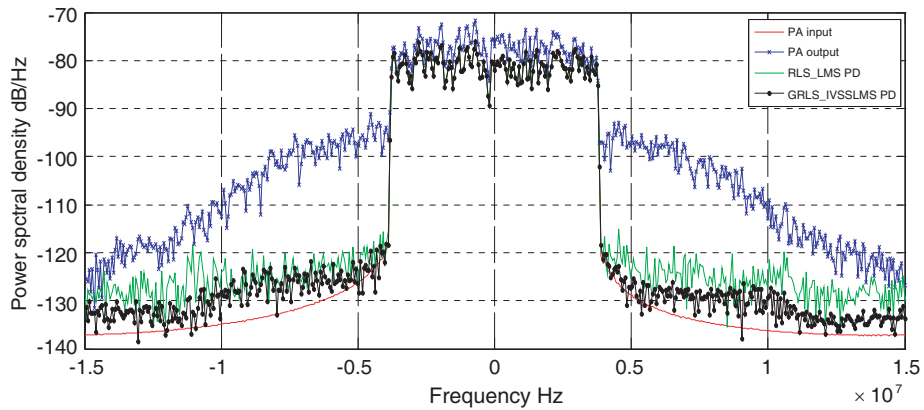


Figure 7. Spectrum comparison chart after the GRLS_IVSSLMS PD algorithms.

GRLS_IVSSLMS PD algorithm is improved by approximately 29 dB compared with the predistortion PA output.

In Figure 8, the AM/AM and AM/PM of the power amplifier before non-predistortion are very poor, and the points are very scattered. However, after the predistortion of GRLS_IVSSLMS algorithm, the AM/AM and AM/PM are basically in a straight line. Compared with LMS and RLS, the linear

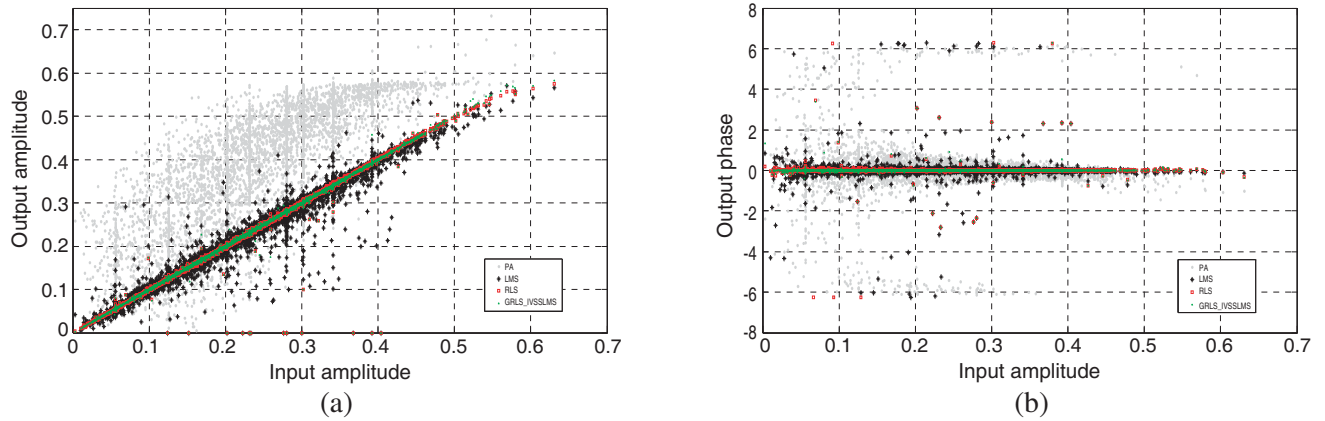


Figure 8. AM/AM and AM/PM characters after the GRLS_IVSSLMS PD algorithm. (a) AM/AM. (b) AM/PM.

Table 1. GRLS_IVSSLMS algorithm performance comparison.

PD algorithm	PLTC PA ($M = 2, N = 5$)	
	EVM (%)	NMSE (dB)
LMS	4.6672	-26.0712
RLS	3.6652	-27.1336
RLS_LMS	1.5440	-35.1256
GRLS_IVSSLMS	1.4032	-37.0742

effect is greatly improved and can meet the system requirements.

In Table 1, compared with the LMS, RLS, and RLS_LMS algorithms, the EVM of the proposed method is improved by 3.26%, 2.26%, and 0.14%, respectively, whereas the NMSE of the proposed method is improved by 11, 9.9, and 1.95 dB, respectively.

5. CONCLUSION

The increasing demand of testing large-scale real-world programs necessitates the automation of the testing process. As a basic problem in software testing, path-wise test data generation is particularly important. We proposed a look-ahead search method in our previous research, and in this paper we make improvements on interval arithmetic, which enforces arc consistency. We analyze, in detail, the working process of interval arithmetic, and based on the analytical result, the iterative operator is introduced and adopted in the constraint solving process, for the purpose of detecting infeasible paths as well as shortening the time consumption. Experimental results prove the effectiveness of the iterative operator and its applicability in engineering.

Our future research will involve how to make interval arithmetic more efficient in arc consistency checking. We will also introduce more arc consistency checking techniques and more ways of representing the values of variables such as affine arithmetic. The MC/DC coverage criterion will be given more emphasis. We will continue to improve the effectiveness of the generation approach and provide better support for more data types.

ACKNOWLEDGMENT

We thank the anonymous reviewers for their feedback and comments.

This work was supported by the National Natural Science Foundation of China Youth Fund Project (No. 61701211), Liaoning Provincial Key Laboratory Funding Project (NO. LJZS007), and Liaoning Provincial Department of education general project (L2015209).

REFERENCES

1. Zhang, L., "Three-dimensional power segmented tracking for adaptive digital pre-distortion," *IEICE Electron. Express*, Vol. 13, 1, 2016, doi: 10.1587/elex.13.20160711.
2. Mkadem, F., et al., "Multi band complexity reduced generalized memory polynomial power-amplifier digital predistortion," *IEEE Trans. Microw. Theory Techn.*, Vol. 64, 1763, 2016, doi: 10.1109/TMTT.2016.2561279.
3. Hammi, O., et al., "Multi-basis weighted memory polynomial for RF power amplifiers behavioral modeling," *IEEE MTT-S International Conf.*, Vol. 1, 2016, doi: 10.1109/IEEE-IWS.2016.7585475.
4. Ba, S. N., K. Waheed, and G. T. Zhou, "Efficient lookup table-based adaptive baseband predistortion architecture for memoryless nonlinearity," *EURASIP Journal on Advances in Signal Processing*, 379249, 2010, doi: 10.1155/2010/379249.
5. Chen, H. H., et al., "Joint polynomial and look-up-table predistortion power amplifier linearization," *IEEE Trans. Circuit System*, Vol. 53, 612, 2006, doi: 10.1109/TCSII.2006.877278.
6. Yang, Z., et al., "PA linearization using multi-stage look-up-table predistorter with optimal linear weighted delay," *IEEE International Conf. Signal Process.*, Vol. 47, 2012, doi: 10.1109/ICoSP.2012.6491529.
7. Kim, J., et al., "Digital predistortion of wideband signals based on power amplifier model with memory," *Electronics Letters*, Vol. 37, 1417, 2001, doi: 10.1049/el:20010940.
8. Morgan, D. R., et al., "A generalized memory polynomial model for digital predistortion of RF power amplifiers," *IEEE Transactions on Signal Processing*, Vol. 54, 3852, 2006, doi: 10.1109/TSP.2006.879264.
9. Yao, S., et al., "A recursive least squares algorithm with reduced complexity for digital predistortion linearization," *IEEE International Conf. Signal Process.*, 4736, 2013, doi: 10.1109/ICASSP.2013.6638559.
10. Mandic, D. P., "A generalized normalized gradient descent algorithm," *IEEE Signal Processing Letters*, Vol. 11, 115, 2004, doi: 10.1109/LSP.2003.821649.
11. Liu, Y. J., et al., "A robust augmented complexity-reduced generalized memory polynomial for wideband RF power amplifiers," *IEEE Trans. on Industrial Electronics*, Vol. 61, 2389, 2014, doi: 10.1109/TIE.2013.2270217.
12. Dawar, N., T. Sharma, R. Darraji, and F. M. Ghannouchi, "Linearisation of radio frequency power amplifiers exhibiting memory effects using direct learning-based adaptive digital predistortion," *IET Communications*, Vol. 10, No. 8, 950–954, May 19, 2016, doi: 10.1049/iet-com.2015.1048.
13. Carusone, A. C., "An equalizer adaptation algorithm to reduce jitter in binary receivers," *IEEE Transactions on Circuits and Systems II: Express Briefs*, Vol. 53, No. 9, 807–811, Sep. 2006, doi: 10.1109/TCSII.2006.881161.
14. Akhtar, M. T., M. Abe, and M. Kawamata, "A new variable step size LMS algorithm-based method for improved online secondary path modeling in active noise control systems," *IEEE Transactions on Audio, Speech, and Language Processing*, Vol. 14, No. 2, 720–726, Mar. 2006, doi: 10.1109/TSA.2005.855829.
15. Mitra, A., M. Chakraborty, and H. Sakai, "A block floating-point treatment to the LMS algorithm: Efficient realization and a roundoff error analysis," *IEEE Transactions on Signal Processing*, Vol. 53, No. 12, 4536–4544, Dec. 2005, doi: 10.1109/TSP.2005.859342.